Journal of Orthopaedic Translation 52 (2025) 265–275

Contents lists available at ScienceDirect

Journal of Orthopaedic Translation

journal homepage: www.journals.elsevier.com/journal-of-orthopaedic-translation

Original article

Promotion of bone-tendon healing after ACL reconstruction using scaffold-free constructs comprising ADSCs produced by a bio-3D printer in rabbit models

Kotaro Higa [a], Daiki Murata [b,*], Chinatsu Azuma [a], Kotaro Nishida [a], Koichi Nakayama [b]

[a] Department of Orthopedic Surgery, Graduate School of Medicine, University of the Ryukyus, 1076 Kiyuna, Ginowan, 901-2720, Japan
[b] Center for Regenerative Medicine Research, Faculty of Medicine, Saga University, 1 Honjyo-machi, Saga, 840-8502, Japan

ARTICLE INFO

Keywords:
Adipose-derived mesenchymal stromal cell
Anterior cruciate ligament reconstruction
Bio-3D printer
Bone-tendon healing
Rabbit model
Regeneration
Scaffold-free
Sharpey's fibre-like tissue
Spheroid
Tubular construct

ABSTRACT

Background/Objective: This study evaluated the impact of adipose tissue-derived mesenchymal stromal cells (ADSCs) on bone-tendon healing in rabbit anterior cruciate ligament (ACL) reconstruction.
Methods: Nineteen mature male Japanese White rabbits underwent bilateral ACL reconstruction. ADSC constructs were implanted in the right femoral bone tunnel of each rabbit (implant group), while the left knee served as the control group without implantation. Nine rabbits were sacrificed at 3 and 6 weeks post-surgery, while the remaining were sacrificed immediately post-surgery. Biomechanical and micro computed tomography evaluations were conducted on six rabbits, while histological observation was performed on the remaining three.
Results: showed: (1) The implant group exhibited a significantly greater failure load than the control group at 3 weeks post-surgery. (2) Initially, the amount of new bone in the femoral tunnel was lower in the implant group at 3 weeks but surpassed that of the control group by 6 weeks. (3) Histological analysis indicated faster bone-tendon healing in the implant group than that of the control.
Conclusion: These findings suggest a positive effect of ADSC constructs on bone-tendon healing post-ACL reconstruction in rabbits. However, further studies using larger animal models must confirm these effects comprehensively.
The translational potential of this article: The method of transplanting a scaffold-free autologous ADSC construct is a technique that can safely and reliably transplant ADSCs to the tendon-bone tunnel interface without using foreign substances. It can be applied to bone-tendon healing in ACL reconstruction surgery and other areas, such as the rotator cuff and Achilles tendon attachment site.

1. Introduction

Anterior cruciate ligament (ACL) injury is a prevalent orthopedic condition among young athletes. Recent estimates suggest that approximately 200,000 ACL reconstructions are performed annually in the United States [1]. Deceleration movements, notably jump landings and sudden directional shifts, are primary causes of ACL injuries [2], which are frequently observed in high-impact sports such as soccer and basketball. The ACL, akin to the tendon, meniscus, and cartilage, exhibits very poor vascular distribution and lacks inherent capacity for tissue regeneration post-injury. ACL ruptures have a very poor self-healing capacity due to the absence of blood clot formation within the ACL wound site because the ACL is located in the knee joint, which is filled with joint fluids [3]. Untreated ACL injuries can progress to knee instability, predisposing individuals to meniscal tears and knee osteoarthritis. Hence, surgical intervention via ACL reconstruction is advised [4]. The reconstruction entails creating bone tunnels in the femur and tibia, through which the semitendinousus tendon, bone-pateller tendon-bone, or quadriceps tendon graft is passed, yielding favourable clinical outcomes [5]. Nonetheless, returning to sports typically requires 8–10 months post-surgery, with early resumption proving challenging. Furthermore, the rate of return to pre-injury athletic proficiency is approximately 50 % [6], partly attributable to the prolonged healing process at the interface between the bony tunnel and the grafted tendon [7].

Recently, stem cells derived from various tissues, including bone

* Corresponding author.
E-mail address: st0358@cc.saga-u.ac.jp (D. Murata).

https://doi.org/10.1016/j.jot.2025.03.019
Received 10 September 2024; Received in revised form 28 February 2025; Accepted 30 March 2025

marrow, synovium, and umbilical cord blood, have been shown to promote bone and/or tendon regeneration [8–10]. Adipose tissue-derived mesenchymal stromal cells (ADSCs), which can be easily collected under local anaesthesia and efficiently isolated and cultured, have been used in regenerative therapies [11,12]. ADSCs maintain a high proliferation rate regardless of age and are expected to have various applications in the field of regenerative medicine [13]. Among those stem cells, ADSCs can be isolated in the greatest abundance and may have the highest proliferation rate in mature animals [14]. Additionally, liposuction, which is used to aspirate adipose tissue (AT), is commonly utilised in the aesthetic field and is a globally accepted surgical technique for obtaining AT [15]. Moreover, ADSCs play an important role in bone-tendon healing by forming bone and tendon through osteogenic and tenogenic differentiation under appropriate microenvironmental stimuli such as bone morphogenetic protein-2 [16]. ADSC-derived exosomes promote the proliferation, migration, and osteogenic differentiation of bone marrow-derived mesenchymal stem cells around bone tunnels and bone formation [17]. Furthermore, studies using several animal models have reported that ADSCs promote bone-tendon healing [18,19]. However, the methods of implanting ADSCs into the bone-tendon junction include injecting the cell suspension or inserting cells mixed with fibrin clots into the bone tunnel, which seem to lack implantation accuracy in arthroscopic ACL reconstruction. This is because even if a suspension of ADSCs is introduced into a defective area in the body, only approximately 60 % survive, while the rest fall off and disappear [20]. Additionally, they struggle to form a three-dimensional structure on their own [20]. Therefore, for future ACL reconstruction, establishing a precise method for implanting ADSCs at the bone-tendon junction is necessary. Furthermore, developing a method to deliver mesenchymal stem cells in a three-dimensional (3D) format is essential to ensure proper cells positioning within the bone tunnel.

We have developed a bio-3D printer for placing cell aggregates (spheroids) on a needle array (Kenzan) to fabricate scaffold-free cell constructs of various shapes. Previous work demonstrated the successful fabrication of cell constructs using different cell types and showed cartilage and bone regeneration in rat, rabbit, pig, horse, and human models [11,21–24]. We aimed to enhance bone-tendon healing post-ACL reconstruction using scaffold-free cell constructs of ADSCs produced with a bio-3D printer. This allows the cells to be arranged into 3D shape in advance and provides mechanical strength as a single structure, making it easier to handle during surgery. Additionally, because cells can be easily placed in the desired location and shape, this method is considered a reliable and highly reproducible implant method [22,25].

In this study, we aimed to fabricate tubular cell constructs using rabbit ADSCs, which were then autologously implanted into bone holes in the femurs of rabbit ACL reconstruction models. We subsequently evaluated bone-tendon fusion at the junction through mechanical and histological assessments.

2. Materials and methods

2.1. Animals

Nineteen mature male Japanese white rabbits (Japan SLC, Shizuoka, Japan), 24 weeks old and weighing 3.55 ± 0.2 kg (range: 3.27–3.97 kg), were utilised in this study. ADSCs were isolated from the interscapular fat tissue of each rabbit, and ADSC constructs were prepared according to Section 2.2. Among the 38 knees from 19 animals, the right knee was assigned to the implant group, where the ADSC constructs was implanted during ACL reconstruction, and the left knee was assigned to the control, where only ACL reconstruction was performed without implanting the ADSC construct. Nine rabbits were evaluated 3 weeks after surgery (n = 9 for the implant group and n = 9 for the control group), and nine rabbits were evaluated 6 weeks after surgery (n = 9 for the implant group and n = 9 for the control group). Six of each group underwent micro-computed tomography (μCT) evaluation immediately after being sacrificed, followed by biomechanical evaluation, while the remaining three underwent histological evaluation. In addition to these comparison subjects, one of the 19 animals was sacrificed immediately after surgery, and a histological evaluation of the bone tunnel after ACL reconstruction was performed as a reference case (Time 0). The right (implanted) knee was histologically evaluated to determine whether the ADSC construct was properly implanted, and the left (control) knee was evaluated to assess whether the graft was properly transplanted in the bone tunnel. The specific time points of 3 and 6 weeks were chosen for evaluation, because, in previous literature [26], where adipose stem cells were administered after ACL reconstruction in a rabbit model, significant differences occurred in histological and mechanical evaluations at the early stage of 8 weeks after surgery. However, after 8 weeks, bone-tendon healing had progressed in both groups, and the differences disappeared. Therefore, as this study focused on evaluating differences in bone-tendon healing in the early stages after ACL reconstruction, the evaluation periods were set at 3 and 6 weeks. Animal experiments were conducted at the Institute of Animal Care Committee of the University of Ryukyu (approval no. A2019113).

2.2. Isolation and expansion of AT-derived mesenchymal stem cells

Interscapular AT (10 g per animal) was aseptically collected from each rabbit under general anaesthesia, minced, and digested for 3 h in phosphate-buffered saline containing 0.1 % collagenase (Collagenase Type I; Worthington Biochemical, Lakewood, NJ). The digests were filtered through a 70 μm pore membrane (Cell Strainer; BD Biosciences, Franklin Lakes, NJ, USA), and centrifuged at 180×*g* for 5 min at room temperature. After removing the resulting supernatant, the pellet was resuspended in culture medium (CM) consisting of Dulbecco's Modified Eagle's Medium (DMEM; Life Technologies, Carlsbad, CA, USA), 10 % foetal bovine serum (FBS; HyClone FBS, Thermo Scientific, Waltham, MA), and 1 % antibiotics (100 U/mL penicillin G and 100 μg/mL streptomycin; Pen Strep; Life Technologies). The cells were centrifuged for a second time, resuspended in fresh CM, and seeded into 75 cm^2 culture flasks (Iwaki Tissue Culture flasks; AGC Techno Glass Co., Ltd., Shizuoka, Japan). Following incubation at 37 °C with 5 % CO_2 for 5 days at passage 0, adherent cells were harvested using recombinant trypsin (TrypLE Select; Life Technologies). Subsequently, the collected cells with fresh CM were seeded at 8.0×10^5 cells per 150 cm^2 dish (Falcon Tissue Culture Dish, Corning Inc., NY, USA) and cultured until reaching 90 % confluence with a change of medium every other day. This process was repeated three times until passage four to obtain sufficient cells for construct preparation.

2.3. Tri-lineage differentiation assay for AT-derived mesenchymal stem cells

For the osteogenic differentiation assay, fresh CM containing ADSCs was aliquoted into a 6-well plate (Nunc Cell-Culture Treated Multidish, Thermo Fisher Scientific K.K., Tokyo, Japan) at a density of 3.0×10^4 cells/well. After 24 h of incubation, the CM was replaced with an osteogenic induction medium (Differentiation Basal Medium-Osteogenic; Lonza, Walkersville, MD, USA) supplemented with 100 mM ascorbic acid, 10 mM glycerophosphoric acid, and 1 mM dexamethasone. The cells were cultured for 4 weeks, following established protocols [11]. For the chondrogenic differentiation assay, ADSCs in fresh CM were seeded into a 6-well plate at a density of 3.0×10^4 cells/well. After 24 h of incubation, the medium was replaced with a chondrogenic induction medium (Differentiation Basal Medium-Chondrogenic, Lonza), supplemented with 4.5 g/L D-glucose, 350 mM L-proline, 100 nM dexamethasone, and 0.02 g/L transforming growth factor-beta 3. The cells were then cultured for 2 weeks, following previously established procedures [11]. For the adipogenic differentiation assay, fresh ADSCs were resuspended in a 6-well plate at a density of

2.0×10^5 cells/well. Following a 24-h pre-incubation, the medium was replaced with adipogenic induction medium (Lonza), supplemented with 4.5 g/L D-glucose, 100 mM indomethacin, 10 mg/mL insulin, 0.5 mM 3-isobutyl-1-methylxanthine, and 1 mM dexamethasone. The cells were cultured continuously for 1 week, according to previously reported methods [11]. For the negative control of the osteogenic, chondrogenic, and adipogenic differentiation assays, ADSCs were cultured in CM for 4, 2, and 1 week(s) respectively. Subsequently, calcium apatite crystals were assessed using Alizarin Red staining, cartilage-specific proteoglycans were stained with Alcian Blue, and adipocyte-specific intracellular lipids were detected with Oil Red O, as detailed in previous studies [11]. The information of the tri-lineage differentiation assay described previously is summarised in Table 1.

2.4. Bio-3D printing to fabricate tubular cell construct

At least 5×10^6 ADSCs were utilised for the fabrication of each construct. These cells were introduced into three 96-well low-adhesion plates (PrimeSurface 96U Plate; Sumitomo Bakelite, Tokyo, Japan) at a density of 1.7×10^4 cells/well in a medium containing equal amounts of fibroblast growth medium (FGM-2; Lonza) and endothelial cell growth medium (EGM-2; Lonza) regarding the previous report [27]. Following static culture at 37 °C with 5 % CO_2 for 48 h, the cells aggregated to form spheroids, with diameters measuring approximately 580 μm (Fig. 1a). Subsequently, the spheroids were transferred onto a needle array (Kenzan) using a bio-3D printer (Regenova; Cyfuse Biomedical K.K., Tokyo, Japan), as described previously [11,27]. A total of 240 spheroids were positioned on a 9×9 tubular Kenzan to construct a tubular cell construct, as depicted in Fig. 1b–d. Following bio-3D printing, the spheroids on the Kenzan were cultured in a circulating medium at 37 °C with 5 % CO_2 for 10 days to facilitate fusion (Fig. 1e and f). Upon removal from the Kenzan, the construct exhibited an outer diameter of 2.5 mm and a height of 4 mm (Fig. 1g). Subsequently, it was affixed to a 14G catheter tube and autologously implanted into the rabbit ACL reconstruction model (Fig. 1h).

2.5. Histology of tubular cell construct

One of the constructs was fixed in 10 % neutral buffered formalin (NBF) for 1 week and embedded in paraffin. Serial sections (5 μm thick) were placed on glass slides and stained with haematoxylin and eosin (HE), Safranin O, and picrosirius red (PSR). The PSR-stained sections were examined under a polarised light microscope. The sections were used for immunohistochemistry for type I and type II collagen and terminal deoxynucleotidyl transferase deoxyuridine triphosphate nick-end labelling (TUNEL) staining. Goat polyclonal anti-type I collagen antibody (1310-01; Southern Biotechnology Associates Inc, Birmingham, AL, USA) was used as the primary antibody for type I collagen, and goat polyclonal anti-type II collagen antibody (1320-01; Southern Biotechnology Associates Inc) was used as the primary antibody for type II collagen.

2.6. Surgical procedure of ACL reconstruction and construct implantation

Rabbits were pretreated with sedatives (intramuscular injections of 50 mg/kg medetomidine and 250 mg/kg midazolam) and analgesics (intramuscular injections of 100 mg/kg butorphanol and 5 mg/kg ketamine). ACL reconstruction with a semitendinosus tendon autograft was then performed bilaterally under inhalation anaesthesia (2 % isoflurane) and local anaesthesia (1 % lidocaine solution). To prevent postoperative infection, a subcutaneous injection of chloramphenicol (15 mg/kg) was administered on the day of surgery. Surgery was performed after aseptic draping with clean, sterilised sheets. After the bilateral hind limbs were shaved and prepared in a standard sterile manner, the patellofemoral joint was medially incised to expose the native ACL. The ACL was carefully removed from the attachment sites of the femoral and tibial bones, and the semitendinosus tendon was exposed and transected at its proximal musculotendinous insertion. The tendon was prepared as a graft by passing holding sutures through its proximal end without cutting the tibial attachment.

The femoral tunnels, with a diameter of 2.5 mm, were drilled in the lateral femoral condyle, and tibial tunnels, with a diameter of 2 mm, were drilled in the medial aspect of the tibia. Intra-articular holes were created at the original ACL attachment site in both tunnels. The tendon graft was passed through the tibial and femoral tunnels, and two tubular constructs were inserted into the gap between the femoral tunnel and the graft, passing through the lumen of the construct in the right hind limb (implanted knee). The length of the femoral bone tunnel was approximately 8.5 mm. Given that the length of the ADSC construct was approximately 4 mm inserting two ADSC constructs vertically into the bone hole created an environment where the cell construct was in contact with the bone-tendon interface. However, no implantation was performed around the left graft (control knee). Finally, the graft was sutured to the periosteum of the femur using 3-0 nylon with the knee joint flexed at 45°. At 0, 3, and 6 weeks after surgery, the rabbits were sacrificed by a lethal dose injection of pentobarbital. The entire knee was harvested by amputation at the femoral and tibial metaphyses.

2.7. μCT evaluation for ACL reconstruction

The knees of implant and control groups were scanned using a μCT (R_mCT2; Rigaku, Tokyo, Japan) before mechanical examination at 3 or 6 weeks after surgery. The volume of newly formed bone in the femoral tunnel was evaluated using CT 3D images constructed using Amira-

Table 1
Summary of tri-lineage differentiation assay in 6-well plate.

	Cell number (Cell density)	Induction medium composition	Incubation period (Week)	Evaluation method	Evaluation subject
Osteogenic differentiation assay	3.0×10^4 cells/well	Osteogenic induction medium supplemented with 100 mM ascorbic acid, 10 mM glycerophosphoric acid, and 1 mM dexamethasone	4	Alizarin Red staining	Calcium apatite crystals
Chondrogenic differentiation assay	3.0×10^4 cells/well	Chondrogenic induction medium supplemented with 4.5 g/L D-glucose, 350 mM L-proline, 100 nM dexamethasone, and 0.02 g/L TGF-β3[a]	2	Alcian Blue staining	Proteoglycans
Adipogenic differentiation assay	2.0×10^5 cells/well	Adipogenic Induction Medium supplemented with 4.5 g/L D-glucose, 100 mM indomethacin, 10 mg/mL insulin, 0.5 mM IBMX[b], and 1 mM dexamethasone.	1	Oil Red O staining	Intracellular lipids

[a] TGF-β3, transforming growth factor beta 3.
[b] IBMX, 3-isobutyl-1-methylxanthine.

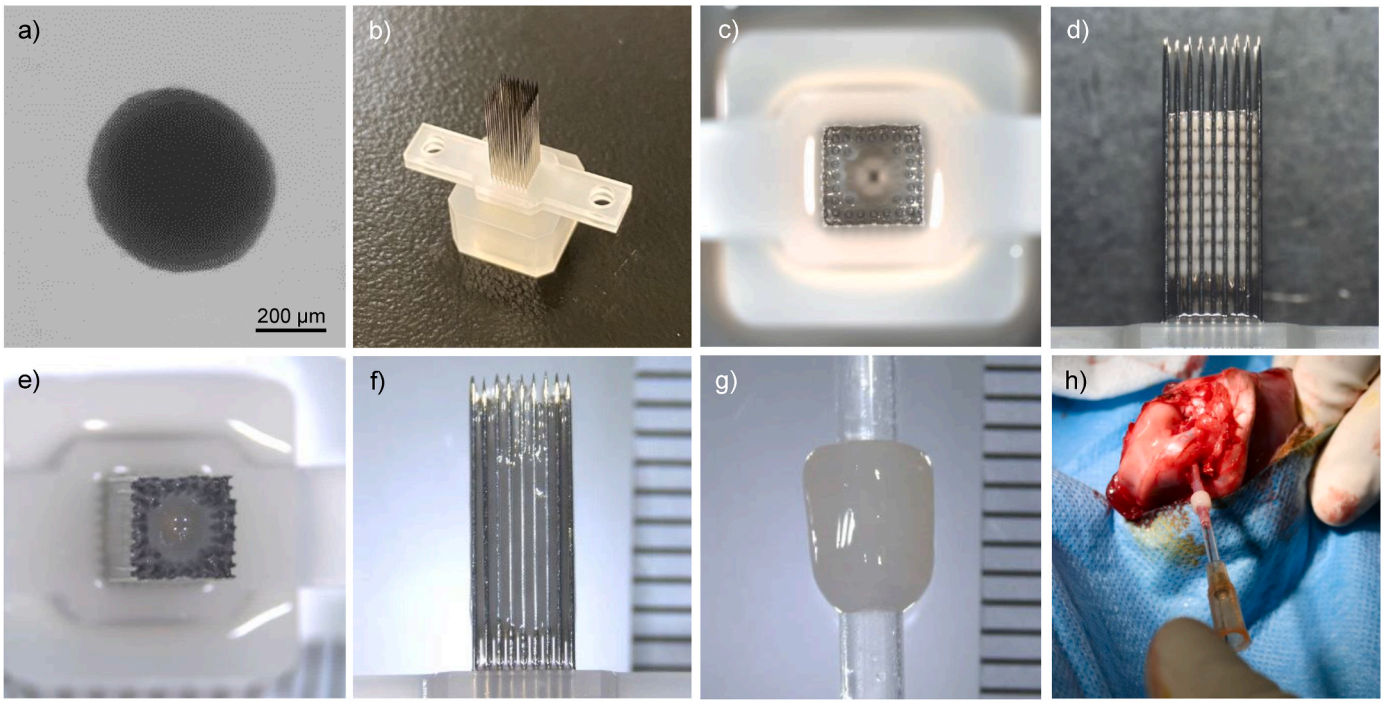

Fig. 1. Preparation of spheroids and tubular constructs. (a) A representative spheroid approximately 580 mm in diameter for use in fabricating a construct by bio-3 dimensional (3D) printing. (b) A 9 × 9 tubular Kenzan is used for the fabrication of tubular constructs. (c, d) A tubular construct fabricated immediately after stacking spheroids onto the needles of a Kenzan. (e, f) A tubular construct cultured on the Kenzan needles for 10 days after fabrication. (g, h) A tubular construct collected from Kenzan and transferred onto the catheter just before implantation.

Avizo Software 2019.3 (Thermo Fisher Scientific, Tokyo, Japan) (Fig. 2a). Cylindrical images, each was a diameter of 2.5 mm, were placed onto the femoral tunnels in the images (Fig. 2b). The overlapping parts of the tunnels were extracted as newly formed bone to calculate its volume (Fig. 2c and d). Data were standardised according to the length of each femoral bone tunnel.

2.8. Mechanical assessment for ACL reconstruction

Mechanical assessment was performed following μCT evaluation at 3 or 6 weeks after surgery. After μCT evaluation, all soft tissues around the knee, except for the tendon graft connecting the femur and tibia, were carefully removed. Next, the 3-0 nylon used for fixing the graft to the periosteum at the time of surgery was removed. The femur and tibia were mounted on a tensile testing machine (AGS-H; SHIMADZU, Kyoto, Japan), and the femur was pulled along the longitudinal axis of the femoral and tibial tunnels at an elongation rate of 2 mm/min in opposite directions. The ultimate load at the point of failure was recorded, and stiffness was calculated as the slope of the linear region of the load-elongation curve between 1.5 mm and 2 mm. The failure pattern of each specimen, occurring either by pullout of the tunnel or mid-substance graft rupture, was observed. Our mechanical assessment was performed based on the mechanical testing methodology used by Liu et al. [26], who conducted a rabbit animal study on bone-tendon healing of the ACL.

2.9. Histological evaluation for ACL reconstruction

One animal (two knees) was evaluated histologically immediately after surgery (Time 0), and three animals (n = 3 per group) from the implant and control groups were evaluated 3 and 6 weeks post-operatively. Tissues were fixed in 10 % NBF for HE staining of Time 0, implant group at 3 and 6 weeks, and control group at 3 and 6 weeks, or in 70 % ethanol for Villanueva Goldner (VG) staining of implant and control groups at 3 and 6 weeks. The samples were cut into 5 μm-thick sections longitudinal to the femoral bone tunnel. Histological evaluation of bone-tendon healing at the interface between the bone tunnel and the tendon graft was conducted using light microscopy.

2.10. Statistical analysis

The average ultimate failure loads, stiffness values, and amount of newborn formation between the implant and control groups were compared using the Mann–Whitney U test. The failure mode of the tensile test was analysed using Fisher's exact test. The significance level was set at $p = 0.05$.

3. Results

3.1. Tri-lineage differentiation assay for AT-derived mesenchymal stem cells

ADSCs underwent Alizarin Red staining after osteogenic induction (Fig. 3a), forming sheet-like structures exhibiting positive staining with Alcian Blue after chondrogenic induction (Fig. 3b). Additionally, upon adipogenic induction, adipocyte-like cells containing small lipid vesicles were obtained, as evidenced by positive staining with Oil Red O (Fig. 3c), consistent with previous reports [11].

3.2. Histology of tubular cell construct

Vertical sections of the tubular cell constructs used for microscopic examination are depicted in Fig. 4. In HE-stained sections, spheroid boundaries were indistinct, with spheroids exhibiting fusion (Fig. 4a–c). Safranin O staining yielded negative results (Fig. 4d–f), mirroring the immunohistochemical staining pattern of type II collagen (Fig. 4g–i). Immunostained sections for type I collagen exhibited similarity to PSR-stained sections (Fig. 4j–l). Polarised light microscopy images of PSR staining displayed enhanced light intensity around the needle pores of the spheroids (Fig. 4m), and magnified images of two distinct regions

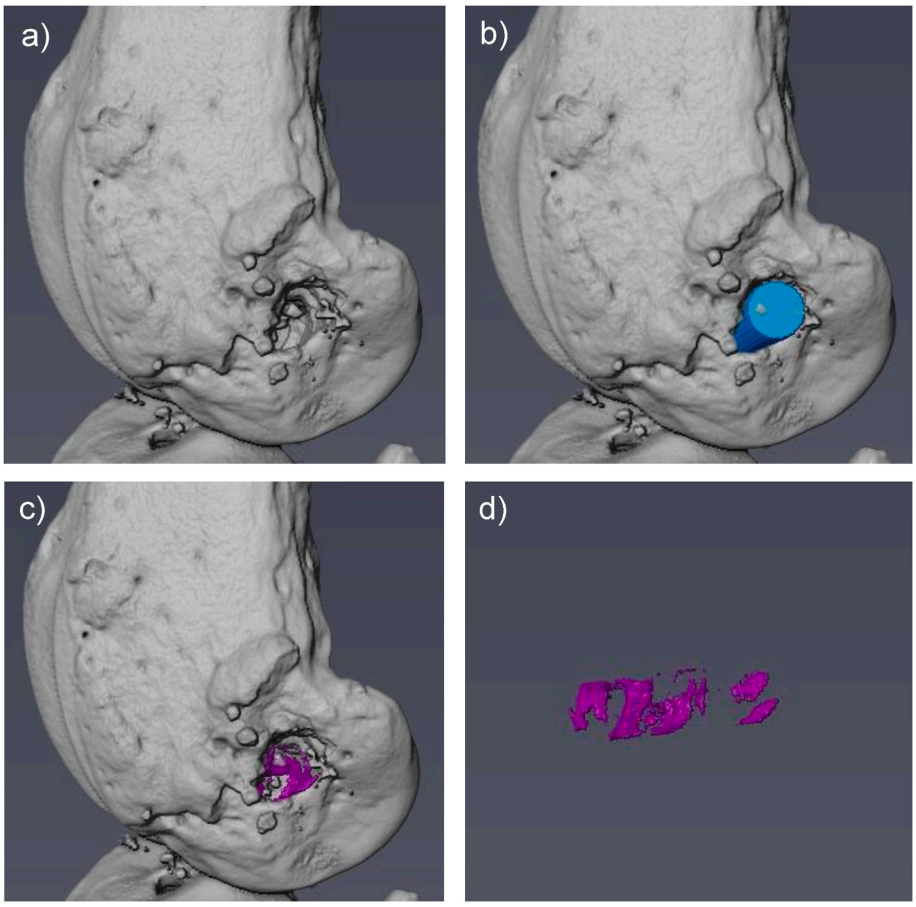

Fig. 2. Micro-computed tomography (CT) to evaluate the volume of new bone formation in the femoral bone tunnel. (a) 3D CT images constructed using Amira-Avizo Software 2019.3 (Thermo Fisher Scientific, Tokyo, Japan). (b) Cylinder images with a diameter of 2.5 mm were placed onto the femoral tunnels and aligned along the axis of the bone tunnel in the images. (c, d) Overlapping parts of the tunnel were extracted as newly formed bone.

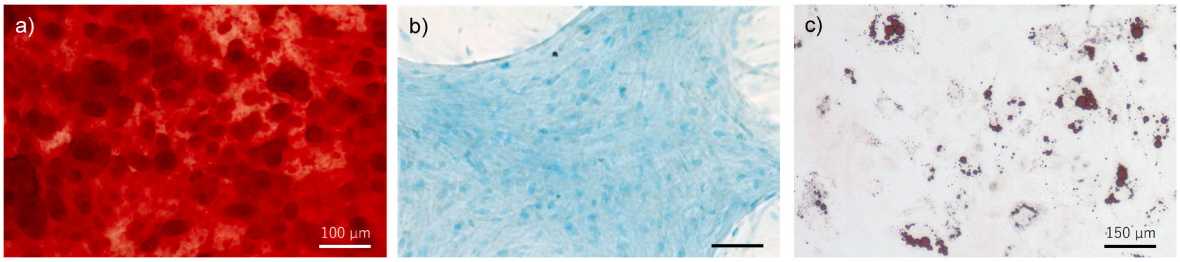

Fig. 3. Tri-lineage differentiation of ADSCs. (a) Calcium apatite stained with Alizarin Red in osteogenic induction. (b) A sheet-like structure positively stained with Alcian Blue in chondrogenic induction. (c) Adipocyte-like cells containing small lipid vesicles stained positively with oil red O in adipogenic induction. Scale bars = 100 μm (a, b) and 150 μm (c).

illustrated the distribution and alignment of collagen fibres encompassing the pores (Fig. 4n and o). Abundant cell nuclei were discernible within the construct, with a few dead cells observed in TUNEL-stained sections (Fig. 4p–r).

3.3. μCT evaluation

The standardised new bone volume in the femoral bone tunnel of the implant group was lower than that of the control group at 3 weeks ($p < 0.01$) (Fig. 5). However, it increased rapidly and exceeded that of the control group at 6 weeks ($p = 0.04$) (Fig. 5).

3.4. Mechanical assessment for ACL reconstruction

3.4.1. Failure pattern under tensile tests

The failure patterns observed in the tensile tests are illustrated in Fig. 6. In the implant group at 3 weeks, five transplanted tendons were pulled out of the femoral tunnels, and one ruptured in the middle. In the control group at 3 weeks, four tendons exited the femoral tunnels, one from the tibial tunnel, and the central portion of one tendon ruptured. At 6 weeks, five tendons ruptured in the mid-substance, and one prolapsed from the tibial tunnel in the implant group. Conversely, in the control group, two tendons were pulled out of the femoral tunnels, two dropped out of the tibial tunnels, and two ruptured in the mid-substance. At both time points, the breaking load in all implanted limbs exceeded that of the controls.

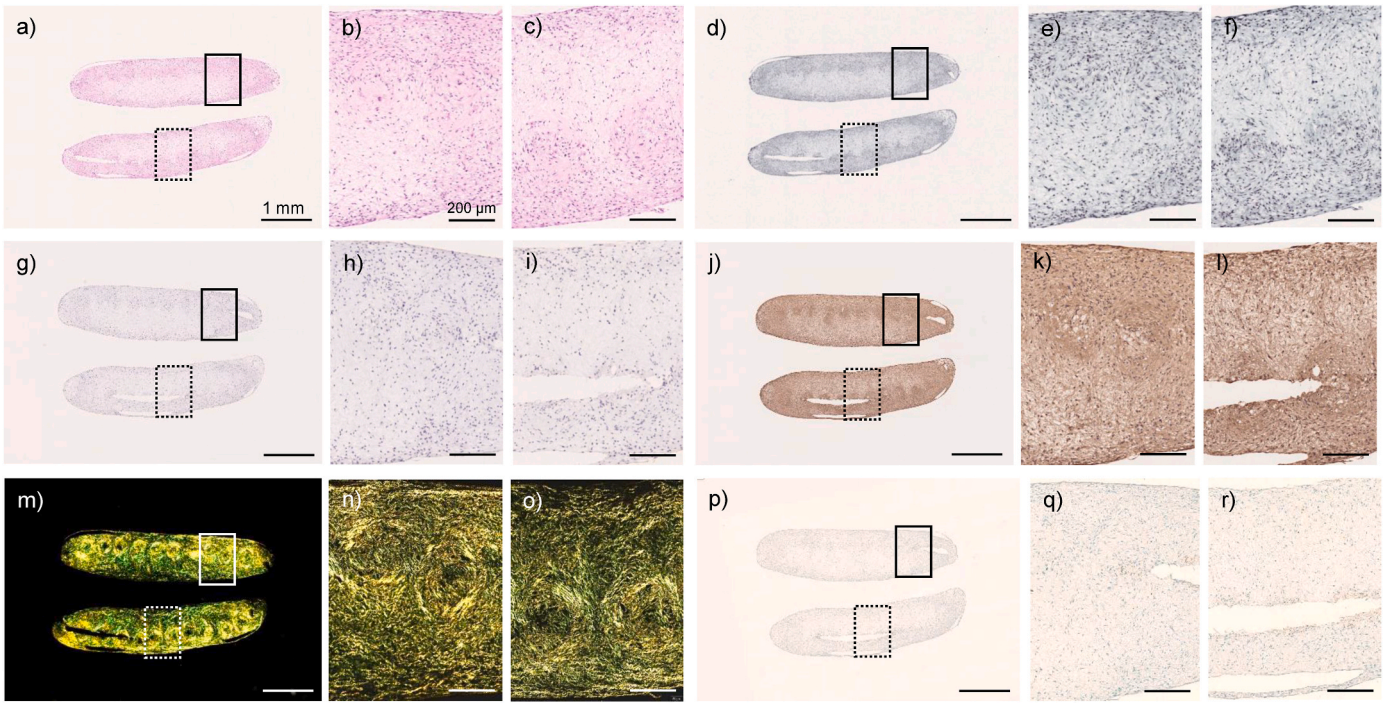

Fig. 4. Representative histology in longitudinal sections of a tubular construct. The sections were assessed using haematoxylin and eosin (a, b, c), Safranine O (d, e, f), immunohistochemistry for type II collagen (g, h, i), immunohistochemistry for type I collagen (j, k, l), picrosirius red observed using a polarised microscope (m, n, o), and TUNEL (p, q, r) staining. The enlargements of solid squares in a, d, g, j, m, and p are b, e, h, k, n, and q, respectively. The enlargements of dotted squares in a, d, g, j, m, and p are c, f, i, l, o, and r, respectively. Scale bars = 1 mm (a, d, g, j, m, p) and 200 μm (b, c, e, f, h, I, k, l, n, o, q, r).

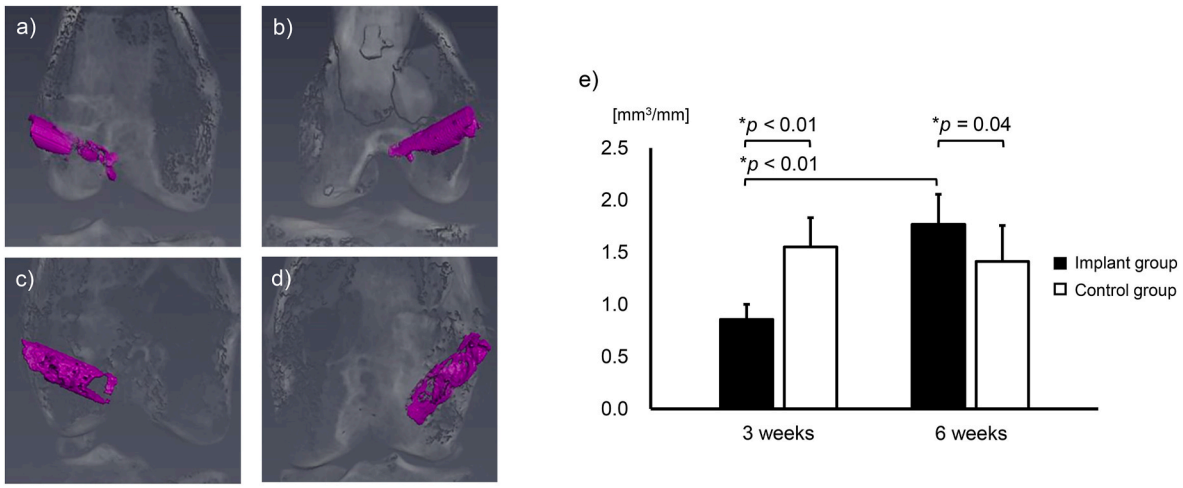

Fig. 5. Micro-computed tomography (CT) evaluation of newly formed bone volume in the femoral bone tunnel. Representative 3D CT images of the implant group at 3 weeks (a), the control group at 3 weeks (b), the implant group at 6 weeks (c), and the control group at 6 weeks (d). (e) The bar chart shows the standardised newly formed bone volume, which was less than that of the control group at 3 weeks ($p < 0.01$). However, it increased rapidly and exceeded that of the control group at 6 weeks ($p = 0.04$).

3.4.2. Ultimate failure loads under tensile tests

The average ultimate failure loads under the tensile tests are represented in Fig. 7a. The average load of the implant group was significantly higher than that of the controls at 3 weeks (35.6 ± 6.5 N vs 21.9 ± 9.0 N, $p = 0.015$). At 6 weeks, the load of the implant group was greater than that of the controls, although there was no significant difference between them (37.2 ± 11.3 N vs. 27.7 ± 9.4 N).

3.4.3. Stiffness under tensile tests

The average stiffness values of the implant group and controls at 3 and 6 weeks are shown in Fig. 7b. No significant differences were observed between the implant group and controls.

3.5. Histological evaluation for ACL reconstruction

3.5.1. Observation of HE staining

Following surgery (Time 0), the construct was observed at the interface between the bone and the tendon grafts in the implanted limb (Fig. 8a and c). Conversely, a noticeable gap was evident between the bone and the tendon graft in the control limb (Fig. 8b and d). By third-week post-operation, in the implant group, the construct had adhered to the tendon graft, and the interface between the construct and bone

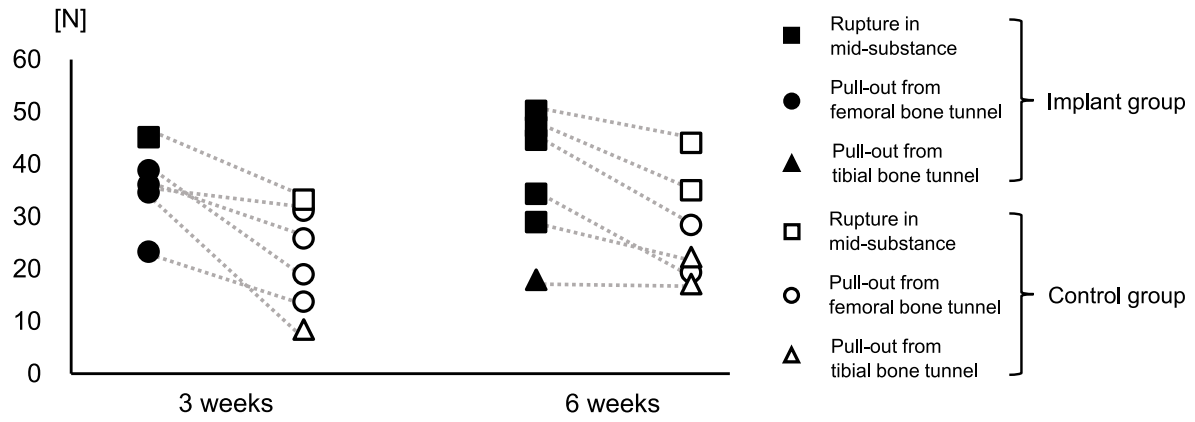

Fig. 6. Point graph showing the ultimate load and failure pattern of each individual under tensile tests of the femur–graft–tibia complex after anterior cruciate ligament reconstruction. The vertical axis of the point graph shows the ultimate load. The square point indicates that the failure pattern was "Rupture in mid-substance", the circle point showed "Pullout from a femoral bone tunnel", and the triangular point indicated "Pullout from a tibial bone tunnel". The points connected by grey dotted lines indicate the right (implanted) and left (control) knees of the same individual.

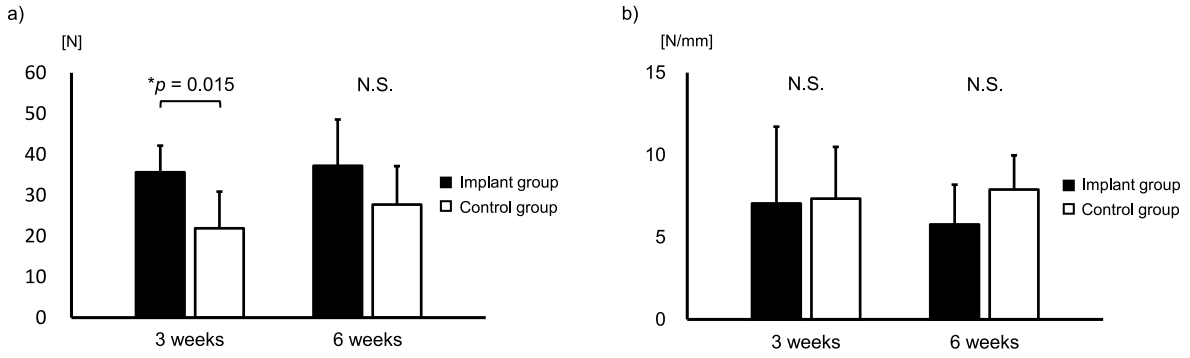

Fig. 7. Ultimate failure load and stiffness under the tensile test of the femur–graft–tibia complex after anterior cruciate ligament reconstruction. (a) Bar chart shows the average failure load under the tensile test. The average load of the implant group was significantly higher than that of the controls at 3 weeks ($p = 0.015$). At 6 weeks, the load of the implant group was greater than that of the controls, although there was no significant difference. (b) Bar chart shows the average stiffness under the tensile test. No significant differences were observed between the implant group and the controls at 3 and 6 weeks.

exhibited fibrous tissue containing numerous cells with spindle-shaped nuclei (Fig. 9a). Conversely, a granulation-like vascular-rich tissue was observed at the interface between the bone and the tendon graft in the control group (Fig. 9b). By the sixth-week post-surgery, the construct was no longer observable, and the bone and the grafted tendon were completely bonded at the interface, where Sharpey's fibre-like tissue was present in the implant group (Fig. 9c, black arrows). Meanwhile, the bone-tendon graft interface was filled with fibrous tissue, and no gap was observed; however, Sharpey's fibre-like tissue was not detected in the control group (Fig. 9d). Heterotopic ossification or bone hyperplasia did not occur inside or outside the joint, and the ligaments and menisci showed no signs of ossification.

3.5.2. Observation of VG staining

Upon VG staining 3 weeks postoperatively, a red-stained osteoid layer was observed at the inner margin of the cancellous bone in contact with the grafted tendon in the implant group (Fig. 10a). Conversely, no periosteum was evident at the bone-tendon interface, and the trabecular bone was exposed in the control group 3 weeks post-surgery (Fig. 10b). At the 6-week mark post-implantation, the periosteum between the bone and grafted tendon exhibited thickening, and the grafted tendon was bridged to the bone by Sharpey's fibre-like tissue (Fig. 10c, white arrows). Moreover, some yellow-green regions, suggestive of young bone, were visible within the organised collagen fibres of the implant group (Fig. 10c). At the bone-tendon interface, a bony layer was evident at the inner margin of the cancellous bone in the control group (Fig. 10d).

4. Discussion

This study describes the initial investigation into the implantation of tubular constructs, composed of rabbit ADSCs, utilising a bio-3D printer equipped with a needle array. The implants were inserted into the gap between the grafted tendon and bone within the femur tunnels, created during ACL reconstruction, aiming to augment the fusion of tendon and bone.

4.1. Characteristics for AT-derived mesenchymal stem cells

AT-derived cells sourced from the interscapular region of rabbits were confirmed to be rabbit ADSCs, possessing osteogenic, chondrogenic, and adipogenic differentiation capabilities, as previously documented [11]. These cells, originally residing in AT, exhibit a notable propensity to differentiate into adipocytes. The adipogenic induction period in this study spanned only seven days, significantly shorter than that required for osteogenic and chondrogenic induction. However, despite this abbreviated timeframe, in vivo differentiation into adipocytes was not observed.

4.2. Characteristics of the tubular ADSC construct

A bio-3D printer can fabricate constructs tailored to the shape and size of individual bone tunnels [27], enabling the creation of constructs that precisely match the tunnel dimensions. The constructs fabricated on Kenzan using the bio-3D printer had a lumen width of approximately

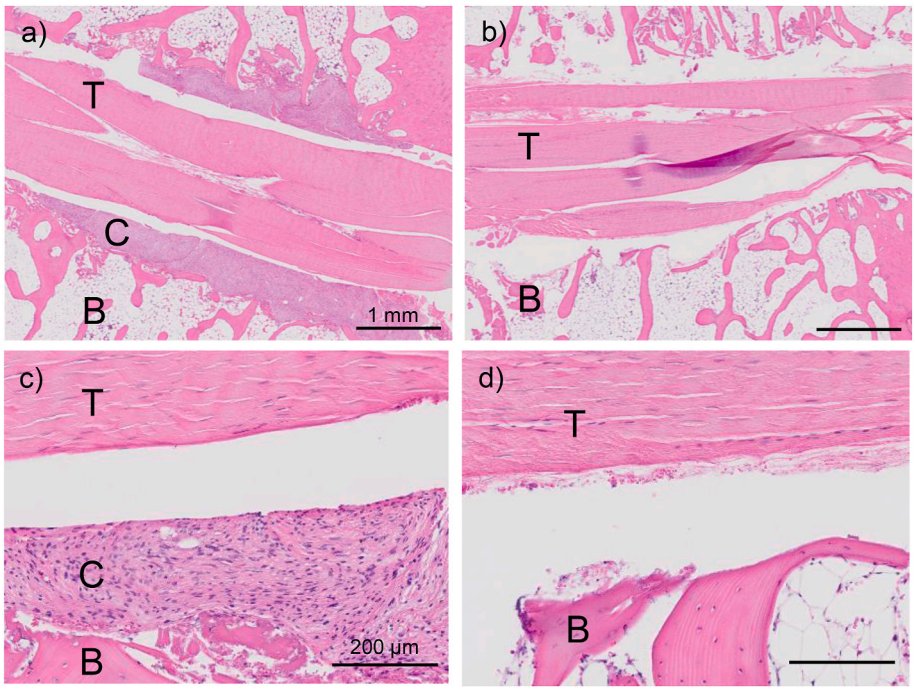

Fig. 8. Representative histology of the longitudinal sections of the femoral bone tunnel in the Time 0 case. The sections were assessed using haematoxylin and eosin staining. The interface between the femoral bone and the tendon graft in the implanted limb (a, c) and the control limb (b, d). T indicates a grafted tendon. C indicates the implanted construct. B indicates tunnelled bone. Scale bars = 1 mm for (a, b), and 200 μm for (c, d).

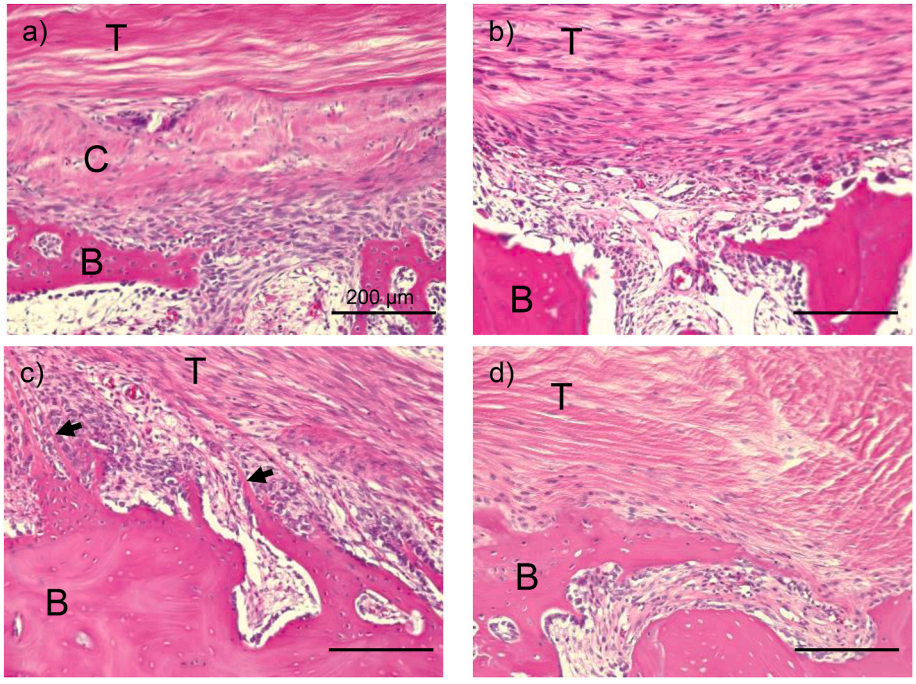

Fig. 9. Representative histology in the longitudinal sections of the femoral bone tunnel. The sections were assessed by haematoxylin and eosin. The interface between the femoral bone and the tendon graft in the implant group at 3 weeks (a), the control group at 3 weeks (b), the implant group at 6 weeks (c), and the control group at 6 weeks (d). T shows a grafted tendon. C shows an implanted construct. B shows tunnelled bone. Black arrows show Sharpey's fibre-like tissue. Scale bars = 200 μm.

2.5 mm; however, the width narrowed upon retrieval from Kenzan and implantation. Additionally, bio-3D printed constructs have been shown to reduce the risk of foreign body reactions and infections compared to grafts fabricated by conventional 3D printers due to the absence of scaffold usage [28]. None of the rabbits in the study experienced foreign body reactions or infections. Moreover, using constructs without scaffolds allows for the implantation of more ADSCs as a single mass, even in tight spaces such as femoral bone tunnels. While the mechanical properties of the constructs were not examined in this study, they proved to be sufficiently stiff and elastic for implantation under surgical procedures using tweezers.

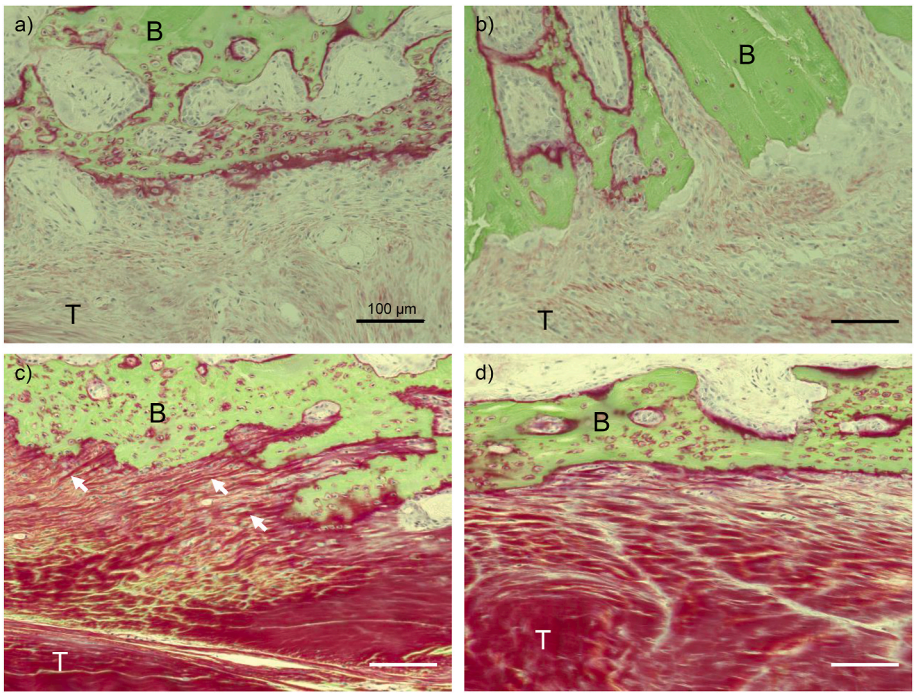

Fig. 10. Representative histology of the longitudinal sections of the femoral bone tunnel, assessed using Villanueva Goldner staining. The interface between the femoral bone and the tendon graft in the implant group at 3 weeks (a), the control group at 3 weeks (b), the implant group at 6 weeks (c), and the control group at 6 weeks (d). T represents a grafted tendon. B represents tunnelled bone. White arrows indicate Sharpey's fibre-like tissue. Scale bars = 100 μm.

4.3. ACL reconstruction and ADSC construct implantation

4.3.1. Ossification of the construct

The μCT evaluation revealed a significantly lower amount of newly calcified bone in the femoral tunnels of the implant group compared to that in the controls 3 weeks post-surgery. Additionally, VG staining performed 3 weeks postoperatively showed an osteoid layer at the inner margin of the trabecular bone at the bone-tendon graft interface in the implant group, which was absent in the control group. These findings indicate that the ADSC construct facilitated bone remodelling at the bone-tendon graft interface in the early stages after implantation by forming an uncalcified/radiolucent bone matrix. Moreover, the quantity of newly calcified bone in the implant group exceeded that in the control group at 6 weeks post-surgery, affirming the continuous promotion of bone remodelling at the bone-tendon graft interface by ADSC constructs and the achievement of complete bone-tendon fusion. One of the histological characteristics of the native enthesis at the bone-tendon interface is the formation of non-calcified and calcified fibrocartilage layers. However, the healing process of the tendon-bone tunnel after ACL reconstruction surgery, which we attempted to recover, differs slightly, with healing proceeding through a so-called indirect healing pattern in which Sharpey's-like fibres appear at the boundary between the bone and tendon [29]. We believe that the presence of the ADSC construct at the bone-tendon interface promoted the formation of earlier Sharpey's-like fibres, contributing to tendon-bone tunnel healing.

The mechanism underlying this phenomenon is believed to involve the differentiation of ADSCs within the construct. By 3 weeks post-implantation, ADSCs are thought to differentiate into chondrocytes within the gap between the bone tunnel and the grafted tendon, subsequently transitioning into osteocytes through the process of endochondral ossification by 6 weeks post-implantation, as previously described [11,12]. Although the detailed mechanism underlying the effect of ADSC construct implantation on bone-tendon fusion in this study remains unclear, Mifune et al. reported that ACL-derived stem cells promote bone-tendon fusion after ACL reconstruction by promoting angiogenesis and osteogenesis to increase the mechanical strength of the bone-tendon connection [30]. Bone marrow stromal cell-derived extracellular matrix has been reported to enhance the osteogenesis of ADSCs [31]. Tendon-derived extracellular matrix promotes the tenogenic differentiation of ADSCs [32], and collagen fibres with a certain orientation accelerate ADSC proliferation and platelet-derived growth factor release from ADSCs [33]. Therefore, ADSCs implanted between the bone and tendon may have undergone osteogenic and tenogenic differentiation in response to the surrounding environment, thus promoting bone-tendon fusion in this study.

4.3.2. Mechanical strength of the connection between tendon and bone

In this study, the therapeutic effects of bio-3D-printed constructs were evaluated using tensile tests. The failure load was significantly greater in the implant group than in the control group 3 weeks after surgery. Histological evaluation simultaneously showed substantial fibrous tissue with numerous spindle-shaped cells in the remaining construct in the implant group, whereas granulation tissue was present in the gap between the bone and tendon in the control group. These results suggest that the bio 3D-printed construct promoted a fibrous union between the bone and tendon 3 weeks after implantation. However, the failure pattern involved withdrawal from the femur in five of the six limbs in the implant group, indicating that a strong union had not been achieved at that time.

Six weeks after surgery, there was no significant difference in the ultimate failure load between the implant and control groups. Histologically, in the control group, at the same time, fibrous tissue was present between the bone and tendon without a gap, although Sharpey's fibre-like tissue was not observed. This absence may explain the mechanical strength improvement of the control group at 6 weeks post-surgery compared to 3 weeks postoperatively. However, one case of separation from the tibia occurred at 3 weeks and two cases at 6 weeks after surgery in the control group, suggesting the possibility of tendon deterioration due to direct contact between the bone and the implanted tendon. Nonetheless, the bone and the grafted tendon were completely bonded at the interface where Sharpey's fibre-like tissue was present 6 weeks after implantation, indicating that bone-tendon fusion progressed

more rapidly in the implant group than in the control. No grafted tendons dropped out of the femur in the implant group 6 weeks after implantation, indicating a strong union.

These results indicate that implanting bio-3D-printed ADSC constructs into the gap between the bone and the grafted tendon during ACL reconstruction significantly affects mechanical stability and boen-tendon fusion in the early stages of post-implantation progress. In the future, this technique could enable earlier initiation of rehabilitation after ACL reconstruction than is currently typical.

4.4. Limitations

This study had a few limitations. First, the mechanical analysis results are subject to biases, encompassing values for the bond strength between the bone and the grafted tendon as well as the tensile strength of the tendon graft itself. However, the observed shift in failure pattern during the tensile test, from "pullout" to "rupture" in the implanted limb, may elucidate the contribution of the ADSC constructs to bone-tendon fusion.

Second, despite the use of rabbits as experimental animals, it is important to acknowledge that the natural healing capacity of small animals differs from that of humans. Therefore, conducting similar experiments in larger animals, such as pigs and dogs, is imperative to comprehensively evaluate their preclinical efficacy.

Third, histological analysis of the grafted tendon itself was not performed because changes in the graft after transplantation were not included in this study. However, further investigation into the remodelling and maturation of the grafted tendon is warranted, as they may significantly influence the mechanical properties of the femur–tendon–tibia complex. Conversely, a previous study demonstrated that the grafted tendon was pulled out from the bone tunnel 12 weeks after transplantation, but subsequently ruptured at the mid-substance of the tendon [34]. Therefore, early bone-tendon fusion is undeniably one of the most pivotal factors in successful ACL reconstruction.

Fourth, the diameters of the tunnels created in the femur were consistent between the implanted and control limbs. Consequently, a gap between the bone and the grafted tendon existed in the control limb, which is not typical in standard ACL reconstruction surgery. To mitigate this limitation, we presented the results of tensile tests conducted with grafts transplanted into tunnels of varying sizes as supplementary information. The ultimate failure load tended to be higher in the implanted limbs during tensile testing, particularly when employing a protocol in which the diameter of the femoral bone tunnel was 3 mm for the implanted limbs and 2 mm for the control limbs. Furthermore, simultaneous ACL reconstruction on both legs, as undertaken in this study, is uncommon.

Fifth, bone-tendon healing exceeding 1.5 months post-implantation was not observed, as this study focused on the early post-transplantation period. Future investigations should extend observation beyond 1.5 months postoperatively to comprehensively understand the healing process.

Sixth, to evaluate new bone formation between the bone and tendon graft, only the volume of new bone within the femoral tunnel was measured globally; the cross-sectional area of the femoral tunnel was not assessed. Consequently, the assessment of bone foraminal enlargement remains incomplete. Nonetheless, the implant and control limbs exhibited new bone formation in this study, suggesting minimal impact on the results.

Seventh, it is unclear whether the results of this experiment are due to the differentiation and formation of the implanted constructs, or whether the surrounding cells repaired the bone and formed Sharpey's fibres using the implanted construct as a scaffold. Therefore, in the future, we will clarify this question by labelling the cells and implanting them into experimental animals to track the behaviour after implantation.

4.5. Conclusion

Tubular constructs made of ADSC spheroids and fabricated by the scaffold-free Kenzan method have the potential to promote bone-tendon integration in the early stage after ACL reconstruction.

5. The Translational Potential of this article

The method of transplanting a scaffold-free autologous ADSC construct is a technique that can safely and reliably transplant ADSCs to the tendon-bone tunnel interface without using foreign substances. It can be applied to bone-tendon healing in ACL reconstruction surgery and other areas, such as the rotator cuff and Achilles tendon attachment site.

Data availability statement

Data will be made available on request.

Credit author statement

Kotaro Higa prepared the paper, obtained the adipose tissues, performed surgery for ACL reconstruction and construct implantation, assessed bone tunnels using μCT, performed the mechanical assessment, evaluated the specimens via histopathology, and interpreted data. Daiki Murata prepared the paper as a corresponding author, organised the study, interpreted the data, isolated and expanded the cells, performed the tri-lineage differentiation assay, created the tubular constructs, assessed the constructs using histology, assisted in surgery for ACL reconstruction and construct implantation, and interpreted the data. Chinatsu Azuma conceived the study, assisted with surgery for ACL reconstruction and construct implantation, and interpreted the data. Kotaro Nishida supervised the study and interpreted the data. Koichi Nakayama conceived, encouraged, and supervised the study and interpreted the data. All authors approved the final version of the manuscript.

Declaration of generative AI and AI-assisted technologies in the writing process

The entire text was originally created by the authors and has been revised by Editage, an English proofreading company; no Generative AI and AI-assisted technologies have been used in the writing process.

Funding/support statement

This study was financially supported by the Okinawa Prefectural Project to Koichi Nakayama and the Japan Society for the Promotion of Science Grants (19K18503 and 22H03204 to Daiki Murata; 22K16769 to Kotaro Higa).

Declartion of conflicts interest

Koichi Nakayama is a co-founder and shareholder of Cyfuse Biomedical K.K. and the External Director of Arktus Therapeutics. The other authors have no commercial, proprietary, or financial interests in the products or companies described in this article.

Acknowledgements

The authors acknowledge the useful advice provided by Drs. Hidetoshi Matsuda, Fuminari Uehara, Takashi Toma, and Hiroki Yabiku. We would like to appreciate Shoko Takao and Miho Miyake for their assistance in culturing the cells and fabricating the constructs. We would also like to thank Ayako Tanaka for her assistance with animal experiments. We also thank the engineers at Thermo Fisher Scientific for providing a

detailed explanation of the 3D CT analysis.

Appendix A. Supplementary data

Supplementary data to this article can be found online at https://doi.org/10.1016/j.jot.2025.03.019.

References

[1] Lynch TS, Parker RD, Patel RM, Andrish JT, Spindler KP, Group MOON. The impact of the multicenter orthopaedic outcomes network (MOON) research on anterior cruciate ligament reconstruction and orthopaedic practice. J Am Acad Orthop Surg 2015;23:154–63. https://doi.org/10.5435/JAAOS-D-14-00005B.

[2] Boden BP, Sheehan FT. Mechanism of noncontact ACL injury. J Orthop Res 2022; 40:531–40. https://doi.org/10.1002/jor.25257.

[3] Kiapour AM, Murray MM. Basic science of anterior cruciate ligament injury and repair. Bone Joint Res 2014;3:20–1. https://doi.org/10.1302/2046-3758.32.2000241.

[4] Segawa H, Omori G, Koga Y. Long-term results of non-operative treatment of anterior cruciate ligament injury. Knee 2001;8:5–11. https://doi.org/10.1016/s0968-0160(00)00062-4.

[5] Samuelsen BT, Webster KE, Johnson NR, Hewett TE, Krych AJ. Hamstring autograft versus patellar tendon autograft for ACL reconstruction: is there a difference in graft failure rate? A meta-analysis of 47,613 patients. Clin Orthop Relat Res 2017;475:2459–68. https://doi.org/10.1007/s11999-017-5278-9.

[6] DeFazio MW, Curry EJ, Gustin MJ, Sing DC, Abdul-Rassoul HA, Ma R, et al. Return to sport after ACL reconstruction with a BTB versus hamstring tendon autograft: a systematic review and meta-analysis. Orthop J Sports Med 2020;8: 2325967120964919. https://doi.org/10.1177/2325967120964919.

[7] Kondo E, Yasuda K, Katsura T, Hayashi R, Kotani Y, Tohyama H. Biomechanical and histological evaluations of the doubled semitendinosus tendon autograft after anterior cruciate ligament reconstruction in sheep. Am J Sports Med 2012;40: 315–24. https://doi.org/10.1177/0363546511426417.

[8] Teng C, Zhou C, Xu D, Bi F. Combination of platelet-rich plasma and bone marrow mesenchymal stem cells enhances tendon-bone healing in a rabbit model of anterior cruciate ligament reconstruction. J Orthop Surg Res 2016;11:96. https://doi.org/10.1186/s13018-016-0433-7.

[9] Matsumoto T, Kubo S, Sasaki K, Kawakami Y, Oka S, Sasaki H, et al. Acceleration of tendon-bone healing of anterior cruciate ligament graft using autologous ruptured tissue. Am J Sports Med 2012;40:1296–302. https://doi.org/10.1177/0363546512439026.

[10] Jang KM, Lim HC, Jung WY, Moon SW, Wang JH. Efficacy and safety of human umbilical cord blood-derived mesenchymal stem cells in anterior cruciate ligament reconstruction of a rabbit model: new strategy to enhance tendon graft healing. Arthroscopy 2015;31:1530–9. https://doi.org/10.1016/j.arthro.2015.02.023.

[11] Murata D, Kunitomi Y, Harada K, Tokunaga S, Takao S, Nakayama K. Osteochondral regeneration using scaffold-free constructs of adipose tissue-derived mesenchymal stem cells made by a bio three-dimensional printer with a needle-array in rabbits. Regen Ther 2020;15:77–89. https://doi.org/10.1016/j.reth.2020.05.004.

[12] Murata D, Fujimoto R, Nakayama K. Osteochondral regeneration using adipose tissue derived-mesenchymal stem cells. Int J Mol Sci 2020;21:E3589. https://doi.org/10.3390/ijms21103589.

[13] Dai R, Wang Z, Samanipour R, Koo KI, Kim K. Adipose-derived stem cells for tissue engineering and regenerative medicine applications. Stem Cell Int 2016;2016: 6737345. https://doi.org/10.1155/2016/6737345.

[14] Pittenger MF, Mackay AM, Beck SC, Jaiswal RK, Douglas R, Mosca JD, et al. Multilineage potential of adult human mesenchymal stem cells. Science 1999;284: 143–7. https://doi.org/10.1126/science.284.5411.143.

[15] Li J, Curley JL, Floyd ZE, Wu X, Halvorsen YDC, Gimble JM. Isolation of human adipose-derived stem cells from lipoaspirates. Methods Mol Biol 2018;1773: 155–65. https://doi.org/10.1007/978-1-4939-7799-4_13.

[16] Wu Z, Yang J, Chong H, Dai X, Sun H, Shi J, et al. 3D-printed biomimetic scaffolds loaded with ADSCs and BMP-2 for enhanced rotator cuff repair. J Mater Chem B 2024;12:12365–77. https://doi.org/10.1039/d4tb01073f.

[17] Tan X, Xiao H, Yan A, Li M, Wang L. Effect of exosomes from bone marrow-derived mesenchymal stromal cells and adipose-derived stromal cells on bone-tendon healing in a murine rotator cuff injury model. Orthop J Sports Med 2024;12: 23259671231210304. https://doi.org/10.1177/23259671231210304.

[18] Kosaka M, Nakase J, Hayashi K, Tsuchiya H. Adipose-derived regenerative cells promote tendon-bone healing in a rabbit model. Arthroscopy 2016;32:851–9. https://doi.org/10.1016/j.arthro.2015.10.012.

[19] Zhang X, Ma Y, Fu X, Liu Q, Shao Z, Dai L. Runx2-modified adipose-derived stem cells promote tendon graft integration in anterior cruciate ligament reconstruction. Sci Rep 2016;6:19073. https://doi.org/10.1038/srep19073.

[20] Nakamura T, Sekiya I, Muneta T, Hatsushika D, Horie M, Tsuji K, et al. Arthroscopic, histological and MRI analyses of cartilage repair after a minimally invasive method of transplantation of allogeneic synovial mesenchymal stromal cells into cartilage defects in pigs. Cytotherapy 2012;14:327–38. https://doi.org/10.3109/14653249.2011.638912.

[21] Fujimoto R, Murata D, Nakayama K. Bio-3D printing of scaffold-free osteogenic and chondrogenic constructs using rat adipose-derived stromal cells. Front Biosci (Landmark Ed.) 2022;27:52. https://doi.org/10.31083/j.fbl2702052.

[22] Yamasaki A, Kunitomi Y, Murata D, Sunaga T, Kuramoto T, Sogawa T, et al. Osteochondral regeneration using constructs of mesenchymal stem cells made by bio three-dimensional printing in mini-pigs. J Orthop Res 2019;37:1398–408. https://doi.org/10.1002/jor.24206.

[23] Murata D, Ishikawa S, Sunaga T, Saito Y, Sogawa T, Nakayama K. Osteochondral regeneration of the femoral medial condyle by using a scaffold-free 3D construct of synovial membrane-derived mesenchymal stem cells in horses. BMC Vet Res 2022; 18:53. https://doi.org/10.1186/s12917-021-03126-y.

[24] Nakamura A, Murata D, Fujimoto R, Tamaki S, Nagata S, Ikeya M. Bio-3D printing iPSCs-derived human chondrocytes for articular cartilage regeneration. Biofabrication 2021;13:044103. https://doi.org/10.1088/1758-5090/ac1c99.

[25] Imamura T, Shimamura M, Ogawa T, Minagawa T, Nagai T, Silwal Gautam S, et al. Biofabricated structures reconstruct functional urinary bladders in radiation-injured rat bladders. Tissue Eng Part A 2018;24:1574–87. https://doi.org/10.1089/ten.TEA.2017.0533.

[26] Liu S, Sun Y, Wan F, Ding Z, Chen S, Chen J. Advantages of an attached semitendinosus tendon graft in anterior cruciate ligament reconstruction in a rabbit model. Am J Sport Med 2018;46:3227–36. https://doi.org/10.1117/0363546518799357.

[27] Murata D, Arai K, Nakayama K. Scaffold-free bio-3D printing using spheroids as "bio-inks" for tissue (re-)construction and drug response tests. Adv Healthc Mater 2020;9:e1901831. https://doi.org/10.1002/adhm.201901831.

[28] Nakayama K. In vitro biofabrication of tissues and organs. In: Forgacs G, Sun W, editors. Biofabrication; micro- and nano-fabrication, printing, patterning and assemblies. Amsterdam: Elsevier; 2013. p. 1–21. https://doi.org/10.1016/B978-1-4557-2852-7.00001-9.

[29] Sato Y, Akagi R, Akatsu Y, Matsuura Y, Takahashi S, Yamaguchi S, et al. The effect of femoral bone tunnel configuration on tendon-bone healing in an anterior cruciate ligament reconstruction: an animal study. Bone Joint Res 2018;7:327–35. https://doi.org/10.1302/2046-3758.75.BJR-2017-0238.R2.

[30] Mifune Y, Matsumoto T, Ota S, Nishimori M, Usas A, Kopf S, et al. Therapeutic potential of anterior cruciate ligament- derived stem cells for anterior cruciate ligament reconstruction. Cell Transplant 2012;21:1651–65. https://doi.org/10.3727/096368912X647234.

[31] Zhang Z, Luo X, Xu H, Wang L, Jin X, Chen R, et al. Bone marrow stromal cell-derived extracellular matrix promotes osteogenesis of adipose-derived stem cells. Cell Biol Int 2015;39:291–9. https://doi.org/10.1002/cbin.10385.

[32] Yang G, Rothrauff BB, Lin H, Gottardi R, Alexander PG, Tuan RS. Enhancement of tenogenic differentiation of human adipose stem cells by tendon-derived extracellular matrix. Biomaterials 2013;34:9295–306. https://doi.org/10.1016/j.biomaterials.2013.08.054.

[33] Cheng XG, Tsao C, Sylvia VL, Cornet D, Nicolella DP, Bredbenner TL. Platelet-derived growth-factor-releasing aligned collagen-nanoparticle fibers promote the proliferation and tenogenic differentiation of adipose-derived stem cells. Acta Biomater 2014;10:1360–9. https://doi.org/10.1016/j.actbio.2013.11.017.

[34] Ekdahl M, Wang JH, Ronga M, Fu FH. Graft healing in anterior cruciate ligament reconstruction. Knee Surg Sports Traumatol Arthrosc 2008;16:935–47. https://doi.org/10.1007/s00167-008-0584-0.